

# Dynamic Test Study of Twelve Elastic Constants of Larch Timber

Qiyun Xu,<sup>a</sup> Xinyuan Lan,<sup>a</sup> Muhammad Ali,<sup>b</sup> Yewei Ding,<sup>a</sup> and Zheng Wang<sup>a,\*</sup>

The elastic modulus, shear modulus, and Poisson's ratio of timber are the elastic constants characterizing its material properties. In this paper, the transient excitation method was used to dynamically measure the 10 elastic constants of the falling larch wood under the condition of the free board and cantilever board, that is, 3 elastic moduli  $E$ , 3 shear moduli  $G$ , and 4 Poisson's ratios  $\mu$ . The other two Poisson's ratios  $\mu$  were derived using the principle of orthogonality. At the same time, the elastic modulus, shear modulus, and Poisson's ratio under static conditions were tested and verified by symmetrical four-point bending, asymmetrical four-point bending, and tensile methods. This study is expected to have good application value and practical significance for timber as an engineering structural material, which is widely used in architecture, decoration, furniture, transportation, musical instruments, and in other fields.

DOI: 10.15376/biores.18.4.7805-7817

Keywords: Larch; Modulus of elasticity; Shear modulus; Poisson's ratio; Dynamic test

Contact information: a: College of Materials Science and Engineering, Nanjing Forestry University, Nanjing, Jiangsu, China; b: College of Civil Engineering, Nanjing Forestry University, Nanjing, Jiangsu, China; \*Corresponding author: wangzheng63258@163.com

## INTRODUCTION

Wood, as an inhomogeneous and orthotropic natural polymer material, differs from other materials in many aspects (Yin 1996). The mechanical properties of wood include the relationship between stress and strain, elasticity, viscoelasticity (plasticity, creep), strength, hardness, *etc.* Its mechanical properties are significantly different from other homogeneous materials (Chui and Smith 1990; Chui 1991; Yoshihara and Sawamura 2006). The elastic modulus, shear modulus, and Poisson's ratio of wood are not only the elastic constants but also the three basic physical properties of wood. The elastic modulus, shear modulus, and Poisson's ratio of wood are the elastic constants that characterize its material properties. The natural frequency of the material is closely related to the three, so there are many research results on the elastic constant of wood and wood composites obtained by dynamic test method (Yoshihara 2009; Wang *et al.* 2014, 2015, 2019; Ponzio *et al.* 2021; Su *et al.* 2021; Zhou *et al.* 2021). As an engineering structural material, the 12 elastic constants of wood are of great significance for its engineering applications and material research. Accurate measurement of the elastic constant of wood is conducive to quality control in the process of wood production and processing, achieving the purpose of accurate grading, and ensuring that the wood produced meets the predetermined standards and requirements. At the same time, it can provide reliable basic data for engineering design to ensure that the designed structure has sufficient strength and stability when stressed. Many researchers used probabilistic methods to study the mechanical properties of materials (Dauletbek *et al.* 2021; Peng *et al.* 2018; Wang and Ghanem 2021, 2022; Wang

2023). Therefore, it is important to adopt convenient and high-precision dynamic test methods (Timothy 1965; Zhang 1992) to carry out the test and research of 12 elastic constants of wood.

The mechanical properties of wood are orthotropic. There are three main directions and three sections. The three main directions are grain direction (L), chord direction (T), and radial direction (R). The three sections are transverse section (RT or TR), radial section (LR or RL), and chord section (LT or TL). According to the mechanical properties of wood, the shear modulus values on the same plane are equal, that is,  $G_{xy} = G_{yx}$ , so the 12 elastic constants are 3 elastic moduli  $E_L$ ,  $E_R$ , and  $E_T$ , 3 shear moduli  $G_{LT}$ ,  $G_{LR}$ , and  $G_{TR}$ , and 6 Poisson's ratios  $\mu_{LT}$ ,  $\mu_{TL}$ ,  $\mu_{LR}$ ,  $\mu_{RL}$ ,  $\mu_{TR}$ , and  $\mu_{RT}$ . Therefore, this paper intends to use the dynamic method to test 10 elastic constants ( $E_L$ ,  $E_R$ ,  $E_T$ ,  $G_{LT}$ ,  $G_{LR}$ ,  $G_{TR}$ ,  $\mu_{LT}$ ,  $\mu_{LR}$ ,  $\mu_{TR}$ , and  $\mu_{RT}$ ). The other two elastic constants,  $\mu_{TL}$  and  $\mu_{RL}$ , are derived according to the orthogonality of wood. At the same time, the elastic modulus, shear modulus, and Poisson's ratio are verified by static tests under symmetric, asymmetric four-point bending, and tensile states.

## EXPERIMENTAL

### Materials

The timber tested in this research was larch (*Larix gmelinii* (Rupr.) Kuzen.), produced in Russia. It has the advantages of straight texture and good dimensional stability in making glued laminated timber. The average air-dry density is  $720 \text{ kg/m}^3$ , and the average moisture content is 10.8%. The size and quantity of test pieces are shown in Tables 1 and 2.

According to the status of the specimen, the methods used in this study can be divided into dynamic test, and static test. The dynamic test contains free board and cantilever board test. The static test was performed to verify the accuracy of the dynamic test results. Symmetrical four-point bending test, asymmetrical four-point bending test, and the tensile test were tested in static tests.

**Table 1.** Specification and Quantity of Dynamic Board Test Pieces

Specimen Name	Size (mm)	Quantity (Piece)
LT board	Length 500, Width 80, Thickness 11	9
LR board	Length 500, Width 80, Thickness 11	9
TR board	Length 188, Width 35, Thickness 7	11
RT board	Length 120, Width 35, Thickness 7	6

**Table 2.** Specification and Quantity of Static Beam Test Specimen

Specimen Name	Specifications (mm)	Quantity (Piece)
LT beam	Length 260, Width 25, Height 20	6
LR beam	Length 260, Width 25, Height 20	6

### Methods

#### *Free board test*

The elastic modulus  $E$  and shear modulus  $G$  of LT and LR board specimens were dynamically measured by the free board state. To keep in a free state, the specimen was suspended with an elastic rope. Then, the accelerometer could obtain the first-order

bending and torsional frequency of the free board by knocking the corner with a hammer. The block diagram of the testing system is shown in Fig. 1.

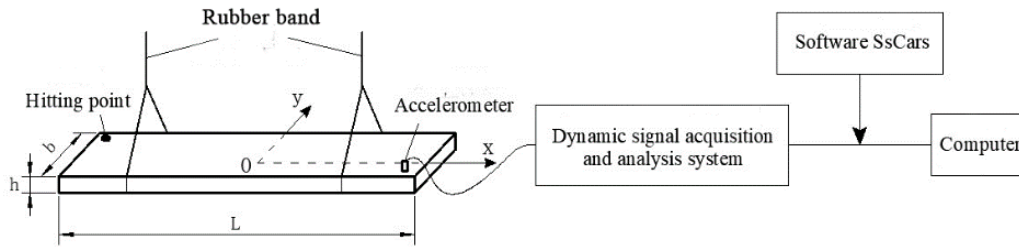


**Fig. 1.** Block diagram of free board test system

The relationship between the elastic modulus  $E$  and the first-order bending frequency  $f_b$  is exhibited in Eq. 1, and the relationship between the shear modulus  $G$  and the first-order torsional frequency  $f_t$  is shown in Eqs. 2 and 3 (Gao *et al.* 2013, 2016),

$$E = 0.9462 \times \frac{\rho f_b^2 l^4}{h^2} \quad (1)$$

where  $\rho$  is the air-dry density of the specimen in  $\text{kg/m}^3$ ;  $f_b$  is the first-order bending frequency in Hz;  $l$  is the length of the test piece in m; and  $h$  is the thickness of the test piece in m. The shear modulus and geometric parameter are given in Eqs. 2 and 3,

$$G = \frac{\pi^2 \rho (l/2)^2 b^2 f_t^2}{7.5 \beta h^2} \quad (2)$$

$$\beta = \frac{1}{16} \left\{ \frac{16}{3} - 3.36 \times \frac{h}{b} \left[ 1 - \frac{1}{12} \left( \frac{h}{b} \right)^4 \right] \right\} \quad (3)$$

where  $\rho$  is the air-dry density of the test specimen in  $\text{kg/m}^3$ ;  $f_t$  is the first-order torsional frequency in Hz;  $l$  is the length of the test piece in m;  $b$  is the width of the test piece in m;  $h$  is the thickness of the test piece in m; and  $\beta$  is the geometric parameter of the board specimen.

#### Cantilever board test

The elastic modulus  $E$ , shear modulus  $G$ , and Poisson's ratio  $\mu$  were obtained by testing RT and TR specimens with cantilever boards as well as Poisson's ratio  $\mu$  of LT and LR larch specimens.

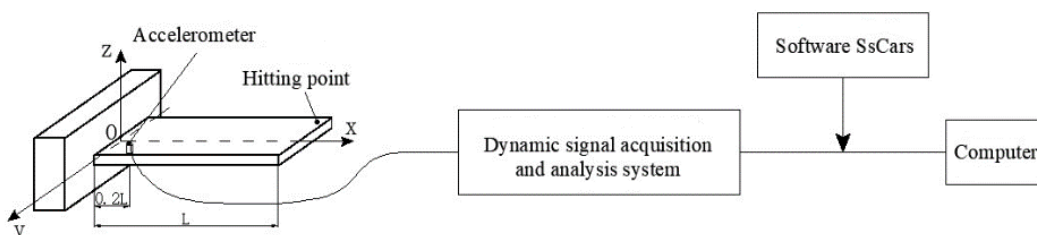


**Fig. 2.** Schematic diagram of cantilever board frequency test

The principle of measuring the elastic modulus of a cantilever board is as shown in Fig. 2: fix the edge of the board specimen to realize the cantilever state, then hit the corner with a hammer, the accelerometer could obtain the dynamic signals.

#### Elastic and shear modulus

According to the transverse vibration beam theory of the beam, the relationship between the first-order bending frequency  $f_b$  of the cantilever beam and the elastic modulus  $E$  is shown in Eq. 4 (Wang *et al.* 2019),

$$E = \frac{48\pi^2}{1.875^4} \cdot \frac{\rho f_b^2 l^4}{h^2} \quad (4)$$

where  $E$  is the elastic modulus of the test specimen (Pa);  $h$  is the thickness of the cantilever board (m);  $\rho$  is the air-dry density ( $\text{kg/m}^3$ );  $f_b$  is the first bending frequency of cantilever board (Hz); and  $l$  is the extension length of cantilever board (m).

The principle of the shear modulus test of the cantilever board is the same as that of the elastic modulus test of the cantilever board. According to the cantilever board torsional mode method, the relationship between the first-order torsional frequency  $f_t$  of the cantilever board and the shear modulus  $G$  is shown in Eq. 5 (Wang *et al.* 2018),

$$G = \frac{\pi^2 \rho l^2 f_t^2}{C_1 \beta h^2} - C_2 E \quad (5)$$

where  $G$  is the shear modulus of the specimen (Pa);  $\rho$  is the air-dry density ( $\text{kg/m}^3$ );  $l$  is the extension length of the cantilever board (m);  $f_t$  is the first-order torsional frequency of cantilever board (Hz);  $h$  is the thickness of cantilever board (m);  $E$  is the elastic modulus of the test piece (Pa);  $C_1$  and  $C_2$  are the vibration mode coefficients of cantilever board;  $\beta = \frac{1}{16} \left[ \frac{16}{3} - 3.36 \frac{h}{b} \left( 1 - \frac{h^4}{12b^4} \right) \right]$  (Wang *et al.* 2016).

The vibration mode coefficient of cantilever board is as follows:

Tangential section:

$$\begin{aligned} C_1 &= 7.3437 + 5.6890b/l - 2.1859h/b \quad (R = 0.9965, n = 16) \\ C_2 &= 0.00482 + 0.04078b/l - 0.03415h/b \quad (R = 0.9885, n = 16) \end{aligned} \quad (6)$$

Scope of application:  $l/b = 2 \sim 5$ ,  $b/h = 5 \sim 13.67$ ;

Radial section:

$$\begin{aligned} C_1 &= 7.4809 + 4.4624b/l - 2.9980h/b \quad (R = 0.9917, n = 16) \\ C_2 &= 0.00763 + 0.04032b/l - 0.05351h/b \quad (R = 0.9638, n = 16) \end{aligned} \quad (7)$$

Scope of application:  $l/b = 2 \sim 5$ ,  $b/h = 5 \sim 13.67$ ;

Cross-section:

$$\begin{aligned} C_1 &= 7.0896 + 6.0212b/l - 0.5121h/b \quad (R = 0.9998, n = 12) \\ C_2 &= -0.0005 + 0.06426b/l - 0.00731h/b \quad (R = 0.9996, n = 12) \end{aligned} \quad (8)$$

Scope of application:  $l/b = 2 \sim 4$ ,  $b/h = 5 \sim 13.67$ .

#### Poisson's ratio

The principle of Poisson's ratio  $\mu$  measurement with a cantilever board is as follows: when the cantilever board in the state of first-order bending vibration, the stress at the vibrating node in the board is in the state of two-dimensional stress.

Taking the cantilever cross section board as an example, in T and R directions, the relationships of the strain  $\varepsilon_T$ ,  $\varepsilon_R$ , and stress  $\sigma_T$ ,  $\sigma_R$  are shown in Eq. 9:

$$\begin{Bmatrix} \varepsilon_T \\ \varepsilon_R \end{Bmatrix} = \begin{bmatrix} \frac{1}{E_T} & -\frac{\mu_{RT}}{E_R} \\ -\frac{\mu_{TR}}{E_T} & \frac{1}{E_R} \end{bmatrix} \begin{Bmatrix} \sigma_T \\ \sigma_R \end{Bmatrix} \quad (9)$$

According to the symmetry principle of the flexibility matrix,  $E_T\mu_{RT} = E_L\mu_{TR}$ . The first letter of the subscript of the  $\mu$  indicates the stretching direction, that is, the length direction of the cantilever board, and the second letter indicates the contraction direction, that is, the width direction of the cantilever board. Therefore,  $\mu_{TR}$  indicates that stretching along the T direction causes contraction in the R direction, and  $\mu_{TR} = -\varepsilon_R/\varepsilon_T$ .

According to Eq. 9:

$$\begin{aligned} \sigma_T &= \frac{E_T}{1 - \mu_{TR}\mu_{RT}} (\varepsilon_T - \mu_{RT}E_R) \\ \sigma_R &= \frac{E_L}{1 - \mu_{RT}\mu_{TR}} (\varepsilon_R - \mu_{TR}E_T) \end{aligned} \quad (10)$$

When  $\sigma_T = 0$ ,  $-\varepsilon_T/\varepsilon_R = \mu_{RT}$ , *i.e.*,  $\mu_{RT} = -\varepsilon_T/\varepsilon_R$ . When  $\sigma_R = 0$ ,  $-\varepsilon_R/\varepsilon_T = \mu_{TR}$ , *i.e.*,  $\mu_{TR} = -\varepsilon_R/\varepsilon_T$ .

Similarly, by analyzing the relationship between strain  $\varepsilon_L$ ,  $\varepsilon_R$ , and stress  $\sigma_L$ ,  $\sigma_R$  in L and R directions of radial section, it can be concluded that when  $\sigma_R = 0$ ,  $\mu_{LR} = -\varepsilon_R/\varepsilon_L$ .

According to the analysis of the relationship between strain  $\varepsilon_L$ ,  $\varepsilon_T$ , and stress  $\sigma_L$ ,  $\sigma_T$  in L and T directions of the tangential section, when  $\sigma_T = 0$ ,  $\mu_{LT} = -\varepsilon_T/\varepsilon_L$ .

Therefore, the relationship between Poisson's ratio and strain in two directions is shown in Eq. 11,

$$\mu_{ji} = -\varepsilon_i / \varepsilon_j \quad (11)$$

where  $\mu$  is Poisson's ratio;  $\varepsilon$  is strain;  $j$  is the length direction of the cantilever board;  $i$  is the width direction of the cantilever board.

It can be seen from the above analysis that Poisson's ratio can be calculated by sticking a cross strain rosette at the  $\sigma = 0$  position.

The elastic modulus  $E$ , shear modulus  $G$ , and Poisson's ratio  $\mu$  of the larch board can be measured synchronously by pasting the 0 to 90° strain gauge and the accelerometer on the cantilever board. The test system block diagram is shown in Fig. 3. The schematic diagram of strain gauge pasting is displayed in Fig. 4. Figure 5 exhibits the sense of the cantilever board test.

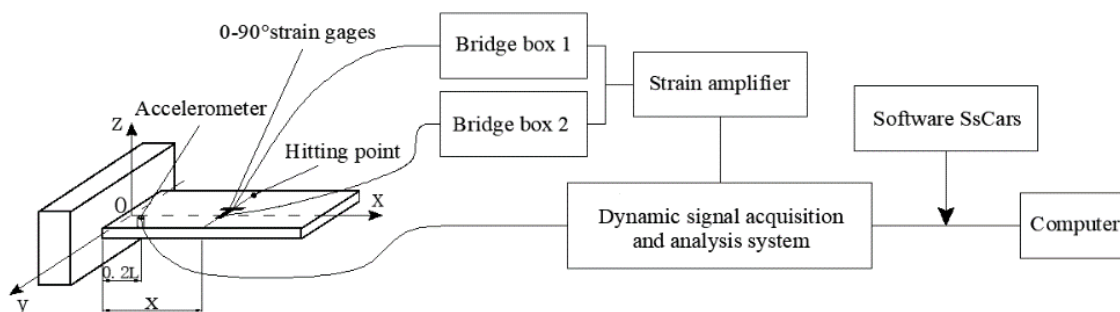
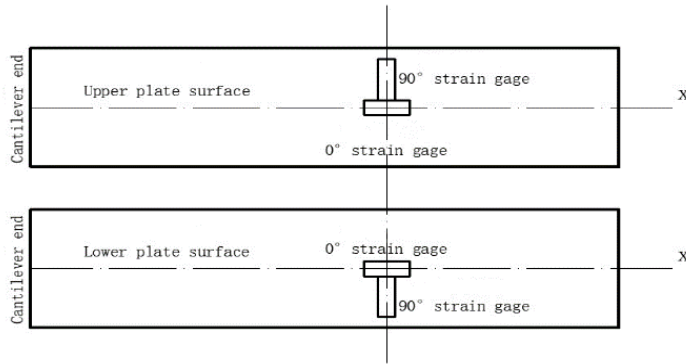
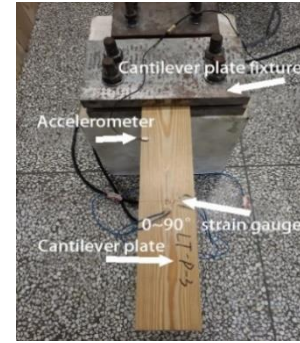


Fig. 3. Block diagram of larch cantilever board test system



**Fig. 4.** Schematic diagram of strain gauge pasting



**Fig. 5.** LT-P-3 Test piece

#### *Four-point bending static test*

In this paper, static four-point bending test was conducted on LT and LR specimens. Yoshihara's asymmetric four-point bending test (Yoshihara and Kubojima 2002; Yoshihara and Suzuki 2005) was used to test the shear modulus  $G$ . The elastic modulus  $E$  can be obtained by symmetrical four-point bending loading test when adjusting loading position on the base of asymmetric four-point bending test.

The  $0^\circ$  and  $90^\circ$  ( $0$  to  $90^\circ$ ) strain gauges were pasted at the midspan of the two opposite planes to be tested for larch beam specimen, as shown in Fig. 6.

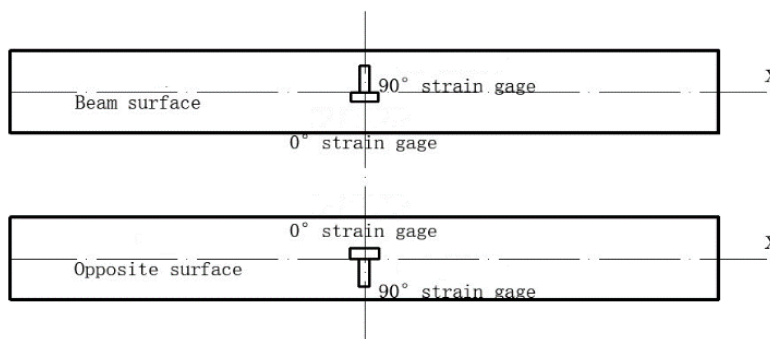


**Fig. 6.** Schematic diagram of beam specimen patch

In the symmetrical four-point bending test, the support span is proposed as  $L$ , the plane where the strain gauge is located is parallel to the ground, and the distributive girder is placed on the  $1/3 l$  of the beam span. As shown in Fig. 7, the weight was placed on the distribution beam for loading. At this time, the  $1/3$  section in the middle of the span was a pure bending section. When loaded, the bottom of the beam is tensioned, and the top is compressed. According to the stress-strain relationship, the weight is loaded step-by-step, and the mean value of strain difference  $\bar{\epsilon}_{0^\circ}$  is obtained from the strain reading of  $0^\circ$  gauge, the static elastic modulus of the beam specimen in the main direction can be obtained by substituting into Eq. 12,

$$E = 8.33 \times \frac{l}{bh^2 \bar{\epsilon}_{0^\circ}} \times 10^6 \quad (12)$$

where  $l$  is the length of the test piece (m);  $b$  is the width of the test piece (m);  $h$  is the thickness of the test piece (m);  $\bar{\varepsilon}_{0^\circ}$  is the mean value of symmetrical four-point bending strain difference of the  $0^\circ$  piece ( $\mu\varepsilon$ ).

The support span of the base was adjusted to  $2/3L$ , and the beam specimen was rotated  $90^\circ$  around the long axis and placed on the support. The plane where the strain gauge is located is perpendicular to the ground. At the same time, the  $2/3 L$  long distribution beam is placed at the other end of the beam. The asymmetric four-point bending state is realized, as shown in Fig. 8. When the weight is loaded on the distribution beam, the beam surface where the strain gauge is located is sheared. According to the stress-strain relationship, the mean value of strain difference  $\bar{\varepsilon}_{0-90^\circ}$  is obtained from the strain reading of  $0$  to  $90^\circ$  gauge, substituting into Eq. 13, the shear modulus of the plane where the strain gauge is located can be obtained,

$$G = 3 \times \frac{20.825}{hb^4 \bar{\varepsilon}_{0-90^\circ}} \times 10^6 \quad (13)$$

where  $l$  is the length of the test piece (m);  $b$  is the width of the test piece (m);  $h$  is the thickness of the test piece (m);  $\bar{\varepsilon}_{0-90^\circ}$  is the mean value of strain difference of  $0$  to  $90^\circ$  unsymmetrical four-point bending gauge ( $\mu\varepsilon$ ).

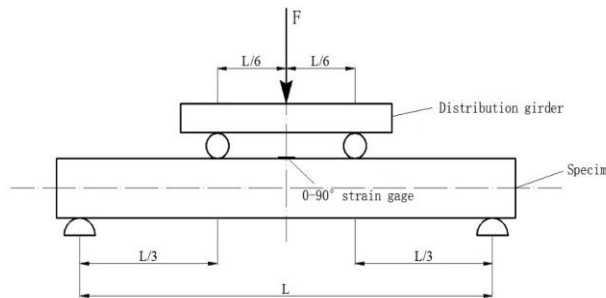


Fig. 7. Symmetrical four-point bending

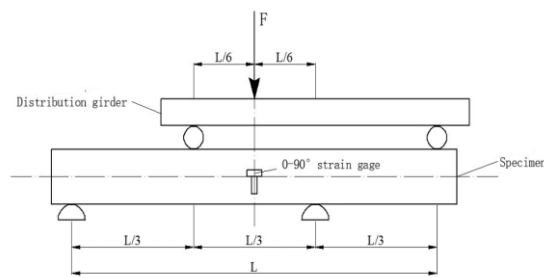


Fig. 8. Asymmetric four-point bending

### Tensile test

Because the Poisson's ratio  $\mu$  cannot be measured by the four-point bending test, the nondestructive specimen in four-point bending test is tensile tested to measure its Poisson's ratio  $\mu$ , and verify the elastic modulus  $E$ .

The highest and lowest loads were determined through pre-testing. The lowest load was  $F_1$  and the highest load was  $F_2$ . The strain values of  $0^\circ$  and  $90^\circ$  pieces corresponding to the lower limit load were respectively  $\varepsilon_{0^\circ}$  and  $\varepsilon_{90^\circ}$ , the strain values of  $0^\circ$  and  $90^\circ$  pieces corresponding to the upper limit load were  $\varepsilon_{0^\circ}$  and  $\varepsilon_{90^\circ}$ , acquired by TDS system. The elastic modulus of the tensile test can be obtained from Eq. 14, and Poisson's ratio can be obtained from Eq. 15:

$$E = \frac{(F_2 - F_1)l}{bh\Delta l} \quad (14)$$

$$\mu = - \frac{\varepsilon_{90^\circ}^i - \varepsilon_{90^\circ}}{\varepsilon_{0^\circ}^i - \varepsilon_{0^\circ}} \quad (15)$$

## RESULTS AND DISCUSSION

### Free Board Test

One bending frequency and one torsion frequency of the board specimen were measured in turn and were substituted into Eqs. 1 to 3 to obtain their respective elastic modulus  $E$  and shear modulus  $G$ . The  $E_L$  and coefficient of variation of LR free board test were 16200 MPa and 6.84%, respectively, and the mean value and coefficient of variation of  $G_{LR}$  were 1320 MPa and 7.17%, respectively. The  $E_L$  and coefficient of variation of LT free board test were 17900 MPa and 6.07%, respectively, and the mean value and coefficient of variation of  $G_{LT}$  were 964 MPa and 8.57%, respectively. The variation coefficients of elastic modulus and shear modulus measured by LR board and LT board were within 10%, and the data results were judged to be suitably accurate and reliable. The  $E_L$  measured by LR board was 9.5% smaller than that measured by LT board, which is within the acceptable technical range.

### Cantilever Board Test

According to the previous research, the position of the strain gauge of the isotropic board specimen at different aspect ratios (Wang *et al.* 2016) is shown in Table 3.

**Table 3.** Attachment Position of Strain Gauge of Cantilever Board Test Piece

Specimen Orientation	Cantilever Length $l$ (mm)	Width $b$ (mm)	Aspect Ratio ( $l/b$ )	Distance between Strain Gauge and Fixed Support End $x$ (mm)	Paste Position $x/l$
TR	105	35	3	16.0	0.15
RT	70	35	2	45.5	0.65
LR	400	80	5	200.0	0.50
LT	400	80	5	204.0	0.51

According to the cantilever test results of LT, LR, TR, and RT boards, the  $\mu_{LT}$  mean value and coefficient of variation of cantilever LT board test were 0.39 and 13.28%, respectively. The mean and coefficient of variation of  $\mu_{LR}$  of cantilever LR board test were 0.37 and 11.2%, respectively. The mean value and coefficient of variation of  $E_T$  of cantilever TR board test were 999 MPa and 4.52%, the mean value and coefficient of variation of  $G_{TR}$  were 128 MPa and 10.66%, and the mean value and coefficient of variation of  $\mu_{TR}$  were 0.41 and 12.71%, respectively. The mean and variation coefficient of  $E_R$  of cantilever RT board test were 1490 MPa and 19.25%, respectively, whereas the mean and variation coefficient of  $G_{RT}$  were 153 MPa and 7.73%. The mean and variation coefficient of  $\mu_{RT}$  were 0.62 and 7.04%, respectively. Clearly, the variation coefficients of elastic modulus  $E$ , shear modulus  $G$ , and Poisson's ratio  $\mu$  obtained from the dynamic test of cantilever board were mostly not more than 15%. The variation coefficient of  $E_R$  measured from RT board was high, reaching 19.2%. This was attributed to the fact that the size of RT board used for testing was relatively smaller than the boards in other directions.

In the cantilever test, the  $G_{TR}$  measured by the TR board was 128 MPa, while the  $G_{RT}$  measured by the RT board was 153 MPa. The difference between the  $G_{TR}$  and  $G_{RT}$  was up to 16%. This is due to the fluctuation of the grain has a greater effect on the small specimen size.

Calculated from test results of cantilever LT, LR, TR, and RT board:  $E_R \times \mu_{TR} = 1490 \times 0.41 = 610.9$ ,  $E_T \times \mu_{RT} \approx E_R \times \mu_{TR}$ . Thus, the data obtained from dynamic test of larch cross-section met the requirement of orthogonal anisotropy. Further,  $\mu_{TR} = 0.41 < \left(\frac{E_T}{E_R}\right)^{\frac{1}{2}} = 0.82$ ,  $\mu_{RT} = 0.62 < \left(\frac{E_R}{E_T}\right)^{\frac{1}{2}} = 1.22$ , meeting Maxwell's law (Wang *et al.* 2003).

### Four-point Bending Test

According to the static four-point bending test results of elastic constants and shear modulus of LT and LR beams, the mean value and coefficient of variation of  $E_L$  measured by symmetric four-point bending method of LT beams were 18,800 MPa and 3.65%, respectively. The mean value and coefficient of variation of  $E_L$  measured by LR beam symmetric four-point bending method were 21100 MPa and 11.0%, respectively. The mean value and coefficient of variation of  $G_{LT}$  measured by LT beam asymmetric four-point bending method were 1005 MPa and 5.39%, respectively. The mean value and coefficient of variation of  $G_{LR}$  measured by LR beam asymmetric four-point bending method were 1307 MPa and 13.4%, respectively. Clearly, the elastic modulus measured by LT specimen was approximately 89% of that measured by LR specimen. Due to the small cross-section and RT direction of the specimen, the error between the two is 11%. The coefficient of variation of  $E_L$  and  $G_{LT}$  specimens measured by LT specimens were 3.65% and 5.39%, respectively. While that of  $E_L$  and  $G_{LT}$  specimens measured by LR specimens were 11.0% and 13.4%, respectively. This indicates that the mechanical properties of these LT specimens were more stable than those of LR specimens in this research.

### Dynamic and Static Test Results and Discussion

The results of the dynamic and static tests in this research are listed in Tables 4 and 5.

**Table 4.** Test Results of Elastic Constants

Specimen Orientation	Test Status	Test Method	Elastic Modulus	Modulus of Shear	Poisson's Ratio
LT direction	Dynamic	Free test	$E_L$ (MPa)	$G_{LT}$ (MPa)	$\mu_{LT}$
		Cantilever test	17859	964	—
	Static	Symmetrical four-point bend	—	—	0.39
		Asymmetrical four-point bend	18759	—	—
		Tensile test	—	984	—
		Tensile test	18337	—	0.40
LR direction	Dynamic	Free test	$E_L$ (MPa)	$G_{LR}$ (MPa)	$\mu_{LR}$
		Cantilever test	16179	1325	—
	Static	Symmetrical four-point bend	—	—	0.37
		Asymmetrical four-point bend	21101	—	—
		Tensile test	—	1307	—
		Tensile test	18982	—	0.36
TR direction	Dynamic	Cantilever test	$E_T$ (MPa)	$G_{TR}$ (MPa)	$\mu_{TR}$
RT direction	Dynamic	Cantilever test	999	128	0.41
			$E_R$ (MPa)	$G_{RT}$ (MPa)	$\mu_{RT}$
			1490	153	0.62

**Table 5.** Dynamic and Static Test Result Error Table

Elastic Constant	Dynamic Results	Static Results	Dynamic/Static
$E_L$	17859 MPa	18660 MPa	95.71%
$E_T$	999 MPa	—	—
$E_R$	1490 MPa	—	—
$G_{LT}$	964 MPa	984 MPa	97.97%
$G_{LR}$	1325 MPa	1307 MPa	101.38%
$G_{TR}$	128 MPa	—	—
$\mu_{LT}$	0.39	0.40	97.50%
$\mu_{LR}$	0.37	0.36	102.78%
$\mu_{TR}$	0.41	—	—
$\mu_{RT}$	0.62	—	—

The elastic modulus of the dynamic free board measured in LT direction was 17900 MPa, and the elastic modulus measured in LR direction was 16200 MPa. The value measured in LR direction was slightly smaller, approximately 90.6% of the value measured in LT direction. Ideally, since both the principal directions are parallel to the grain, the elastic modulus values measured in the LT and LR directions should be equal, and the values measured in this study differ by nearly 10%. This phenomenon is mainly attributed to the different wood grain forms of the two specimens. Because the static elastic modulus in L direction is more than 18000 MPa, the dynamic test result of the elastic modulus in L direction was 17900 MPa.

The shear modulus in TR direction was measured by the dynamic cantilever board as 128 MPa, and that in RT direction was 153 MPa. The value measured in TR direction was small, approximately 83.7% of that in RT direction. Ideally, since the shear planes were the same, the measured shear modulus values in the TR and RT directions should be equal, while the values measured in the TR and RT specimens in this study differ by nearly 17%. Considering that the difference of wood grain will lead to the change of elastic constants (Viguier *et al.* 2017), and the size of TR and RT samples is small, the influence of wood grain on elastic constants becomes larger. Because the size of TR board (105 mm  $\times$  35 mm  $\times$  7 mm) is larger than the size of RT board (70 mm  $\times$  35 mm  $\times$  7 mm), the effect of wood grain fluctuation is relatively small, so the data measured by TR board was selected.

Four static L-direction elastic modulus values were measured, including 18800 MPa measured by symmetrical four-point bending of LT direction specimen, 18300 MPa measured by tensile test of LT direction specimen, 21100 MPa measured by symmetrical four-point bending of LR direction specimen, and 19000 MPa measured by the tensile test of LR direction specimen. Except that the data measured by symmetrical four-point bending of LR direction specimen is too large, the other three data were relatively close because the LR direction data measured by symmetrical four-point bending was too large. Therefore, the static L direction elastic modulus took 18660 MPa as the mean value of tensile test results of LT and LR direction specimens.

It can be seen from Table 5 that the dynamic radial test errors of L direction elastic modulus, LT-direction shear modulus, LT-direction shear modulus, LT-direction Poisson's ratio, and LT direction Poisson's ratio were all within 5%. Compared with the 17% coefficient of variation in the dynamic test conducted by other research (Arriaga *et al.* 2012), the results of dynamic test in this study can be judged to be relatively reliable.

It can be obtained from the dynamic test results that  $E_T \times \mu_{RT} = 619.4 \text{ MPa} \approx E_R \times \mu_{TR} = 610.9 \text{ MPa}$ , so the orthogonality test was consistent. Therefore, based on

orthogonality, the formula  $E_L \times \mu_{TL} = E_T \times \mu_{LT}$  and  $E_R \times \mu_{LR} = E_L \times \mu_{RL}$ , find  $\mu_{TL} = 0.02$ ,  $\mu_{RL} = 0.03$ . Since then, 12 elastic constants of larch specimens based on dynamic test have been obtained.

## CONCLUSIONS

1. This article introduced methods for obtaining the 12 elastic constants of wood dynamically. Compared with traditional static methods, the difference of 10 elastic constants obtained by the dynamic test, including free board test and cantilever board test, was less than 5%, which shows the reliability of these dynamic methods.
2. Based on the 10 elastic constants obtained from the dynamic test, the other 2 elastic constants were derived using the orthogonality principle. Thus the 12 elastic constants of larch specimens can be accurately obtained. In the commonly used method,  $\mu$  would be evaluated in a static test, and other dynamic methods could test  $E$  and  $G$  at a time (Pommier *et al.* 2013). The method proposed in this research could test  $E$ ,  $G$ , and  $\mu$  at a time, with a high accuracy. This could reduce the test time and cost.
3. The dynamic methods introduced in this study could quickly test the 12 elastic constants of larch specimens, conveniently, accurately, reliably, and non-destructively, which is conducive to its popularization, as well as having practical significance for driving the development of related industries.

## ACKNOWLEDGMENTS

### Conflict of Interest

The authors have no competing interests to declare that are relevant to this article.

### Funding Declaration

No funding was received to assist with the preparation of this manuscript.

### Date and Code Availability

All relevant data are within the paper.

## REFERENCES CITED

- Arriaga, F., Íñiguez-González, G., Esteban, M., and Divos, F. (2012). "Vibration method for grading of large cross-section coniferous timber species," *Holzforschung* 66(3), 381-387. DOI: 10.1515/hf.2011.167
- Chui, Y. H. (1991). "Simultaneous evaluation of bending and shear moduli of wood and the influence of knots on these parameters," *Wood Science and Technology* 25, 125-134.
- Chui, Y. H., and Smith, I. (1990). "Influence of rotatory inertia, shear deformation and support condition on natural frequencies of wooden beams," *Wood Science and Technology* 24, 233-245. DOI: 10.1007/BF01153557
- Dauletbek, A., Li, H. T., Xiong, Z. H., and Lorenzo, R. (2021). "A review of

- mechanical behavior of structural laminated bamboo lumber,” *Sustainable Structures* 1(1), article ID 000004. DOI: 10.54113/j.sust.2021.000004
- Gao, Z. Z., Cao, Y., and Chen, X. (2013). “Study of actually measured sawn timber elastic modulus with two dynamic methods,” *Forestry Machinery & Woodworking Equipment* 41(4), 18-20.
- Gao, Z. Z., Wang, Z., and Zhang, X. (2016). “The frequency method for measurement and evaluation of shear modulus of *Picea sitchensis* soundboard,” *China Forest Products Industry* 43(2), 23-26.
- Peng, Y. B., Wang, Z. H., and Ai, X. Q. (2018). “Wind-induced fragility assessment of urban trees with structural uncertainties,” *Wind & Structures* 26(1), 45-56.
- Pommier, R., Breysse, D., and Dumail, J.-F. (2013). “Non-destructive grading of green Maritime pine using the vibration method,” *European Journal of Wood and Wood Products* 71(5), 663-673. DOI: 10.1007/s00107-013-0727-y
- Ponzo, F. C., Antonio, D. C., Niela, L., and Nigro, D. (2021). “Experimental estimation of energy dissipated by multistorey post-tensioned timber framed buildings with anti-seismic dissipative devices,” *Sustainable Structures* 1(2), article ID 000007. DOI: 10.54113/j.sust.2021.000007
- Su, J. W., Li, H. T., Xiong, Z. H., and Lorenzo, R. (2021). “Structural design and construction of an office building with laminated bamboo lumber,” *Sustainable Structures* 1(2), article ID 000010. DOI: 10.54113/j.sust.2021.000010
- Timothy, C. K. (1965). *Mechanical Vibrational Science*, China Machine Press, Beijing, China, pp. 316-333.
- Viguier, J., Bourreau, D., Bocquet, J. F., Pot, G., Bléron, L., and Lanvin, J. D. (2017). “Modelling mechanical properties of spruce and Douglas fir timber by means of X-ray and grain angle measurements for strength grading purpose,” *European Journal of Wood and Wood Products* 75(4), 527-541. DOI: 10.1007/s00107-016-1149-4
- Wang, L. Y., Lu, Z. Y., and Shen, S. J. (2003). “Study on twelve elastic constant values of *Betula platyphylla* Suk. wood,” *Journal of Beijing Forestry University* 25(6), 64-67.
- Wang, Z. H., Wang, Z., Wang, B. J., Wang, Y., Liu, B., Rao, X., Wei, P., and Yang, Y. (2014). “Dynamic testing and evaluation of modulus of elasticity (MOE) of SPF dimensional lumber,” *BioResources* 9(3), 3869-3882. DOI: 10.15376/biores.9.3.3869-3882
- Wang, Z. H., Gao, Z. Z., Wang, Y. L., Cao, Y., Wang, G., Liu, B., and Wang, Z. (2015). “A new dynamic testing method for elastic, shear modulus and Poisson’s ratio of concrete,” *Construction and Building Materials* 100, 129-135. DOI: 10.1016/j.conbuildmat.2015.09.060
- Wang, Z., Gao, Z. Z., and Wang, Y. L. (2016). “Dynamic measuring Poisson’s Ratio  $\mu_{LT}$ ,  $\mu_{LR}$  and  $\mu_{RT}$  of lumbers by electrical method,” *Scientia Silvae Sinicae* 52(8), 104-114. DOI: 10.11707/j.1001-7488.20160813
- Wang, Z. H., Wang, Y. L., and Cao, Y. (2016). “Measurement of shear modulus of materials based on the torsional mode of cantilever board,” *Construction and Building Materials* 124, 1059-1071. DOI: 10.1016/J.CONBUILDMAT.2016.08.104
- Wang, Z., Xie, W. B., Wang, Z. H., and Cao, Y. (2018). “Strain method for synchronous dynamic measurement of elastic, shear modulus and Poisson’s ratio of wood and wood composites,” *Construction and Building Materials* 182, 608-619. DOI: 10.1016/j.conbuildmat.2018.06.139

- Wang, Z., Fu, H. Y., Ding, Y. W., Cao, Y., and Wang Y. L. (2019). “Dynamic testing of shear modulus and elastic modulus of oriented strand board,” *Scientia Silvae Sinicae*, 55(8), 136-146.
- Wang, Z., Xie, W. B., Lu, Y., Li, H. T., Wang, Z. H., and Li, Z. (2019). “Dynamic and static testing methods for shear modulus of oriented strand board,” *Construction and Building Materials* 216, 542-551. DOI: 10.1016/j.conbuildmat.2019.05.004
- Wang, Z. H., and Ghanem, G. (2021). “An extended polynomial chaos expansion for PDF characterization and variation with aleatory and epistemic uncertainties,” *Computer Methods in Applied Mechanics and Engineering* 382, article ID 113854. DOI: 10.1016/j.cma.2021.113854
- Wang, Z. H., and Ghanem, R. (2022). “A functional global sensitivity measure and efficient reliability sensitivity analysis with respect to statistical parameters,” *Computer Methods in Applied Mechanics and Engineering* 402, article ID 115175. DOI: 10.1016/j.cma.2022.115175
- Wang, Z. H., Hawi, P., Masri, S., Aitharaju, V., and Ghanem, R. (2023). “Stochastic multiscale modeling for quantifying statistical and model errors with application to composite materials,” *Reliability Engineering and System Safety* 235, article ID 109213. DOI: 10.1016/j.ress.2023.109213
- Yin, S. C. (1996). *Wood Science*, China Forestry Publishing House, Beijing, China.
- Yoshihara, H. (2009). “Edgewise shear modulus of plywood measured by squareboard twist and beam flexure methods,” *Construction and Building Materials* 23, 3537-3545. DOI: 10.1016/j.conbuildmat.2009.06.041
- Yoshihara, H., and Kubojima, Y. (2002). “Measurement of the shear modulus of wood by asymmetric four-point bending tests,” *Wood Science* 48, 14-19.
- Yoshihara, H., and Suzuki, A. (2005). “Shear stress/shear strain relation of wood obtained by asymmetric four-point bending test of side-tapered specimen,” *Journal of Testing & Evaluation* 33, 55-60. DOI: 10.1520/JTE11936
- Yoshihara, H., and Sawamura, Y. (2006). “Measurement of the shear modulus of wood by the square-board twist method,” *Holzforschung* 60, 543-548. DOI: 10.1515/HF.2006.090
- Zhang, L. M. (1992). *Vibration Test and Dynamic Analysis*, Aviation Industry Press, Beijing, China, pp. 123-230.
- Zhou, Y. H., Huang, Y. J., Sayed, U., and Wang, Z. (2021). “Research on dynamic characteristics test of wooden floor structure for gymnasium,” *Sustainable Structures* 1(1), article ID 000005. DOI: 10.54113/j.sust.2021.000005

Article submitted: July 28, 2023; Peer review completed: September 16, 2023; Revised version received and accepted: September 22, 2023; Published: October 2, 2023.

DOI: 10.15376/biores.18.4.7805-7817